ECMWF RE-ANALYSIS ERA

ERA-40 Project Report Series

11. High clouds over oceans in the ECMWF 15-year and 45-year re-analyses

Frédéric Chevallier, Graeme Kelly, Adrian J. Simmons,
Sakari Uppala and Angeles Hernandez

European Centre for Medium-Range Weather Forecasts
Europäisches Zentrum für mittelfristige Wettervorhersage
Centre européen pour les prévisions météorologiques à moyen terme

Series: ECMWF ERA-40 Project Report Series

A full list of ECMWF Publications can be found on our web site under:
http://www.ecmwf.int/publications/

Contact: library@ecmwf.int

European Centre for Medium Range Weather Forecasts
Shinfield Park, Reading, RG2 9AX, England

ERA-40 Project Report Series No. 11

High clouds over oceans in the ECMWF 15-year and 45-year re-analyses

Frédéric Chevallier, Graeme Kelly, Adrian J. Simmons, Sakari Uppala and Angeles Hernandez

Research Department

December 2003

Submitted to J. Climate

Abstract

The re-analysis programmes of numerical weather prediction (NWP) centres provide global, comprehensive descriptions of the atmosphere and of the Earth surface over long periods of time. The high realism of their representation of key NWP parameters, like temperature and winds, implies some realism for less emblematic parameters, such as cloud cover, but the degree of this realism needs to be documentated.

This study aims to evaluate the high clouds over open oceans in the ECMWF 15-yr and 45-yr re-analyses. The assessment is based on a new 23-yr climatology of monthly frequencies of high cloud occurrence retrieved from the infrared radiances measured by operational polar satellites. It is complemented by data from the International Satellite Cloud Climatology Project.

It is shown that the 45-yr ECMWF re-analysis dramatically improves on the previous 15-yr re-analysis for the realism of seasonal and interannual variations in high clouds, despite remaining systematic errors. More than 60% of the observed anomalies during the January 1979 - February 2002 period in large oceanic basins are captured by the latest re-analysis. However the realism of the analyses in the areas and in the years with sparse observations appears to be poor. Consequently, the interannual variations may not be reliable before January 1979 in most parts of the world. Possible improvements of the handling of assimilated satellite observations before and after this date are suggested.

1 Introduction

Growing concern about the evolution of the Earth's climate has increased interest in understanding past atmospheric records. Time series of satellite observations are relatively short, but they are an interesting source of information because they cover wide portions of the globe. The measurements of the electromagnetic radiation emitted by the Earth-atmosphere system at wavelengths around 11 and 14 μm that have been operationally made by the polar-orbiting satellites of the National Oceanic and Atmospheric Administration (NOAA) cover an exceptionally long period for satellite data. The initial Vertical Temperature Profile Radiometer (VTPR) was operated on-board four NOAA satellites between November 1972 and February 1979. It was superseded by the High-resolution Infrared Radiation Sounder (HIRS) in October 1978, that provided additional infrared channels and which is still operated today. The next generation, for instance the Atmospheric Infra-Red Sounder (AIRS) launched in 2002 by the National Aeronautics and Space Administration (NASA), achieves a much finer sampling of the infrared spectrum.

The extraction of consistent information about the atmosphere from this historical dataset, in spite of instrument and platform orbit changes, has mobilised considerable efforts (e.g. Susskind et al. 1997 and Scott et al. 1999 for the HIRS record). Very few institutes can afford to integrate these observations together with conventional measurements in a global system. Consequently, the re-analysis programs from the National Centers for Environmental Prediction (NCEP) jointly with the National Center for Atmospheric Research (NCAR), from the Data Assimilation Office (DAO) and from the European Centre for Medium-Range Weather Forecasts (ECMWF) have received much attention. Each program relies on a fixed assimilation and forecasting system for the period that it covers, making it more homogeneous than the operational archives of the numerical weather prediction (NWP) centres. To date, ECMWF has run two re-analysis projects, in partnership with other institutes. The first one covered the December 1978 - February 1994 period (ERA-15, Gibson et al. 1997) and the second one (ERA-40, Simmons and Gibson 2000) extended that period backward to September 1957 and forward to August 2002, using a more advanced data assimilation system.

This study aims to evaluate the realism of the high clouds over open oceans in both ECMWF re-analyses. Following the methodology defined by Chevallier et al. (2001), cloud-affected raw observations from VTPR and HIRS serve as an independent reference for ERA-40, since those observations have not been assimilated. ERA-15 used some of them, but in the form of cloud-cleared radiances. To help the interpretation, monthly

frequencies of high clouds are estimated from the raw radiances with the CO_2-slicing method of Wylie et al. (1994). This product not only serves as a validation reference, but is also of direct climatological significance.

The paper is divided into seven sections. Following the present introduction, section 2 describes the model and satellite data. The frequencies of high clouds directly obtained from the VTPR and HIRS observations are presented in section 3. In section 4 this new dataset, ERA-40 and corresponding data from the International Satellite Cloud Climatology Project (ISCCP, Rossow and Schiffer 1999) are inter-compared. ERA-15 is then evaluated in section 5. A specific assessment of the pre-HIRS period of ERA-40 is presented in section 6. Concluding discussion follows in section 7.

2 The data

2.1 ERA-15 and ERA-40

The ERA-15 and ERA-40 productions were mainly based on systems set up six years apart (1994 and 2000 respectively). Many features denote the scientific and technical progress of the ECMWF forecasting system achieved in between, with significant impact on the skill of NWP (Simmons and Hollingsworth 2002). Their knowledge is not needed to understand the results presented here and the reader is referred to Simmons and Gibson (2000) and to Simmons (2001) for a detailed list of the differences between the two systems in terms of spatial resolution, data assimilation system, advection formulation, physical parameterisations, assimilated observations and external forcing. It is worth mentioning that two prognostic equations described the time evolution of cloud condensate and cloud cover in both forecast models (Tiedtke 1993), but these variables were only diagnosed, since the analysis control variables included vorticity, divergence, surface pressure, wind, temperature and moisture only. Ozone was another control variable for ERA-40 only.

Two previous studies specifically documented some aspects of the quality of the clouds in both re-analyses. Jakob (1999) compared total cloud cover from ERA-15 and ISCCP. Chevallier et al. (2001) used infrared and microwave radiances to evaluate high, medium and low clouds in one year of a preparatory ERA-40 run. For high clouds, they noted a systematic underestimation of their radiative forcing, likely caused by an underestimation of the cloud ice, and a too static intertropical convergence zone (ITCZ). The present study complements that by Chevallier et al. (2001) and is based on the full ERA-40 archive.

2.2 VTPR and HIRS

ERA-15 and ERA-40 illustrate two stages of development of a NWP system. Similarly, VTPR and HIRS bear witness to the evolution of the atmosphere sounding instruments. They share seven similar channels. Six of them have a central wavelength between 13 and 15 μm and allow the retrieval of atmospheric temperature in six corresponding broad layers centered about 30, 60, 100, 400, 600 and 800 *hPa*. The seventh common channel is an 11 μm atmospheric window channel. VTPR also incorporates a 18 μm channel that is sensitive to upper tropospheric humidity. HIRS has twelve other infrared that serve various purposes (Smith et al. 1979). Of interest here is an extra 13 μm channel, whose weighting function peaks about 900 *hPa*.

The spacecrafts that carry those instruments orbit at about 850 *km* altitude from pole to pole and in synchronisation with the sun. The orbits actually drift during the life time of the satellites, in particular for those that were positioned to cross the equator northbound in the local solar afternoon (Price 1991). The series of NOAA satellites that followed one another with VTPR or HIRS on-board, and the drift of their orbits appear in Fig. 1. The drift of NOAA-11 is particularly large. NOAA-11 was brought to a 13:40 LST orbit after launch in

September 1988 and had reached a 21:45 LST orbit by April 2000 when its HIRS instrument failed.

The VTPR ground instantaneous field of view (FOV) is typically an ellipse, whose size is about 57×55 km^2 at nadir and 67×91 km^2 at the end of scan, 30° away from nadir (McMillin et al. 1973). The HIRS spot is typically a circle of 17 *km* diameter at nadir. At the end of the scan, 50° from nadir, the ground FOV covers 58 *km* cross-track by 30 *km* along-track (Kidwell 1998). The HIRS FOV from NOAA-15 and NOAA-16 is slightly larger (Goodrum et al. 2000).

2.3 Radiance calibration

Cloud-affected VTPR and HIRS radiances serve here as a reference for the evaluation of the quality of ERA-15 and ERA-40, and have been extracted from the ERA-40 archive for that purpose. It is therefore useful to summarise the steps of their processing at ECMWF.

Li et al. (2000) and Hernandez et al. (2000) describe the in-house calibration of the VTPR and HIRS (until NOAA-14) radiance counts for ERA-40. NOAA-15 and NOAA-16 radiances were calibrated by the Met Office (UK). The data were further bias-corrected with respect to the NWP first-guess radiance simulations using the method described by Harris and Kelly (2001). The scheme takes into account the biases from the instruments, those from the NWP first-guess fields and those from the radiance model. Its parameters are estimated on a large sample of data, usually covering a couple of weeks, during which the instrument is passively monitored in the NWP system (i.e. during which it is not assimilated).

In order to reduce the data load, only one HIRS spot in four was kept in the ERA-40 system, whereas all VTPR data were used.

2.4 ISCCP

A complementary assessment of the quality of ERA-40 is provided by the ISCCP climatology. As described by Rossow and Schiffer (1999), the latter involves an analysis of the 0.6 and 11 μm radiances observed by imagers on-board operational geostationary and polar-orbiting satellites. The ISCCP radiance calibration procedure is reported by Brest et al. (1997). ISCCP is a comprehensive global dataset of cloud variables at varying spatial and temporal resolutions. Two ISCCP parameters, the monthly high cloud amount and the monthly total cloud amount from the D2 product, are utilized in this study. Data from July 1983 to September 2001 were available at the time of writing.

3 Retrieval of high cloud frequency from VTPR and HIRS

3.1 The retrieval method

Cloud-top pressures are retrieved from VTPR and HIRS radiances using a CO_2-slicing method (e.g. Chahine 1974). The present algorithm was initially developed for HIRS and is described by Wylie et al. (1994). The cloud statistics compiled at Wisconsin University (WU) using this technique have been extensively studied and compared to other climatologies (Wylie et al. 1994, Jin et al. 1996, Wylie and Wang 1997, Wylie and Menzel 1999). The algorithm is summarised as follows.

For each HIRS spot, the temperature profile, the absorbing gas profiles and the surface temperature are defined a priori from an external data source: ERA-40 short-range (3 to 9 hour) forecasts in this study. From these

variables, a radiation model, here the Radiative Transfer for Tiros Operational Vertical Sounder (RTTOV: Eyre, 1991; Saunders *et al.*, 1999), sets up a series of radiation quantities. A preliminary cloud detection is based on the $11\mu m$ window channel: if the difference between the observed and the background clear sky radiance does not exceed some threshold, the spot is declared to be clear. Alternatively, the impact of cloudiness on the radiances in the 13-15μm CO_2 absorption band is modelled by two variables: a cloud top pressure P_{top} and a channel-dependent cloud emissivity $n\varepsilon_\nu$. Scattering is ignored and unit surface emissivity is assumed. If the variations of $n\varepsilon_\nu$ between two spectrally-close channels are neglected, P_{top} and $n\varepsilon_\nu$ are uniquely defined for this pair. The CO_2-slicing algorithm is consequently run for four HIRS channel pairs in the 13-15μm band. A quality control selects the most likely $P_{top}/n\varepsilon_\nu$ association or rejects the retrieval. In the latter case the algorithm returns an estimation based on the sole $11\mu m$ channel assuming unity cloud emissivity $n\varepsilon_\nu$.

The quality of the prior information that sets the temperature in the atmosphere and at the surface obviously plays a crucial role in the quality of the retrieval. In particular, if that prior information is biased, the retrieval will be as well. Consequently, data are processed neither over land nor over sea ice, where the ERA-40 surface temperature is not judged of good enough quality for the retrieval. It may be noted that in this context, the principle of the bias-correction scheme used here, which tackles both instrumental and model biases, is appropriate.

3.2 Extension to VTPR

The application of the algorithm to VTPR is straightforward, except that the information brought by the lowest-peaking $13\mu m$ channel is missing for this earlier instrument. Preliminary results for VTPR indicated that without this channel, some cirrus clouds can be erroneously retrieved in place of low stratus clouds. Consequently, a dummy channel is introduced by taking the mean of the $11\mu m$ and the lowest-peaking $13\mu m$ VTPR channel radiances.

The transition from HIRS to VTPR is illustrated in Fig. 2 with the zonal mean high cloud frequencies for December 1978 over ocean, when both VTPR and HIRS were operated. A high cloud is defined as a cloud whose top pressure is lower than 440 *hPa*. One curve is the standard HIRS retrieval, a second one corresponds to the HIRS one using the VTPR modification and a third one is the VTPR retrieval. Differences are usually less than 5% between the two HIRS curves, which seems acceptable for some applications but possibly not for long-term trend studies. For the latter, it would be desirable that HIRS be processed with the VTPR algorithm. This is not done in the present study.

The VTPR curve differs from the 'reduced-HIRS' one mainly because of different horizontal resolutions of the data. The probability of detecting a cloud increases with the lower-resolution VTPR FOV, which increases the high cloud frequency by about 5% at most latitudes. Unfortunately, the effects of the changes of FOV and channels between VTPR and HIRS add rather than compensate, so that the VTPR zonal means are significantly higher than the HIRS ones. No attempt is made here to make the VTPR and HIRS retrievals converge any further.

3.3 A new database of satellite-based cloud statistics

Cloud top pressure and cloud emissivity retrievals have been performed for the whole ERA-40 VTPR and HIRS archive. Individual retrievals are further classified into three cloud types that follow the ISCCP convention (Rossow and Schiffer 1999): high ($P_{top} < 440$ *hPa*), medium (440 *hPa* $\leq P_{top} < 680$ *hPa*) and low ($P_{top} \geq 680$ *hPa*). Thin (respectively thick) clouds are further defined by infrared optical depths lower (respectively larger) than 1.8. The 1.8 threshold on infrared optical depths may be considered to be equivalent to the 3.6

threshold on visible optical depths used in ISCCP (e.g. Jin et al. 1996).

Monthly frequencies of high-, medium- and low-cloud occurrence over ocean in a regular 2.5° equal angle grid have been compiled separately for each satellite for the periods during which it was assimilated in the ERA-40 system (i.e. the periods during which the radiance bias-correction was set). HIRS viewing angles larger than 41° have been removed, since we found that non-linear variations of the retrieved high cloud occurrence with respect to viewing angle caused excessive weight for them in the monthly statistics. Distinction is also made between ascending and descending orbits.

An interesting illustration of the quality of the dataset is shown in Fig. 3, with the series of monthly high cloud occurrences in three broad latitude bands. Most satellite curves overlap with each other, even those in very different orbits, like NOAA-9 and NOAA-10. This highlights the efficacy of the radiance bias-correction scheme. However, a few outliers can be noticed, most of all the four VTPR satellites (NOAA-2, -3, -4 and -5). As expected, the frequencies from VTPR are higher than those from HIRS, but the individual VTPR curves do not agree with each other. The calibration of the VTPR instrument is challenging for two main reasons. First, since it is the only satellite instrument available, the NWP fields have much lower quality when the instrument is passively monitored, at least in the southern hemisphere. Second, each corresponding NOAA spacecraft actually carried two separate VTPR instruments. These were switched on alternatively and have to be calibrated separately. This is particularly true for the VTPRs on-board NOAA-2, for which the switching occurred every few weeks. Moreover, as can be seem in Fig. 1 and 3, the life time of the NOAA-3 VTPR instruments was very short. Finally, it is known that inappropriate bias coefficients were used in the ERA-40 processing for NOAA-4, which is particularly obvious in Fig. 3b. As a consequence, it is difficult to evaluate the quality of the NOAA-2 and NOAA-5 retrievals.

In the HIRS record, NOAA-8 and the last three platforms (NOAA-14, NOAA-15 and NOAA-16) are the outliers. There is no known reason for this and better agreement could arguably be obtained in a future re-analysis of the data from these satellites. NOAA-14 actually agrees with NOAA-12 after 1 January 1997, on which date the ERA-40 radiance bias-correction coefficients were updated.

In the following the high cloud statistics from all individual instruments are compiled in a single time series by excluding the problematic ones, i.e. all VTPR instruments, NOAA-8, NOAA-14 before 1 January 1997, NOAA-15 and NOAA-16. This new climatology covers the period from January 1979 to February 2002.

3.4 Corresponding definition of high clouds for ERA-15 and ERA-40

Satellite retrievals obviously depend on the sensitivity of the observing instrument. For instance, differences between the Stratospheric Aerosol and Gas Experiment II (SAGE II), ISCCP and the HIRS WU cloud climatologies were attributed to different sensitivities of the respective instruments (Liao et al. 1995, Jin et al. 1996). Therefore the comparison between cloud-top pressure retrievals and simulated cloud profiles is not straightforward. Chevallier et al. (2001) suggested computing the model-equivalent to the observed radiances and to process them with the same cloud retrieval algorithm. This approach serves in this study for the evaluation of some aspects of the ERA-40 short-range forecasts (i.e. between 3 and 9 hours depending on observation time). Radiance computations are performed from a version of RTTOV that has been extended to treat multi-layer cloudiness (Chevallier et al. 2001). Importantly, the cloud optical properties and the cloud overlap scheme are consistent with those of the ECMWF model (Morcrette et al. 2001). This 'HIRS simulator' allows a rigorous evaluation of the model but it involves collocating the model fields and the observations both spatially and temporally. To do this, most of the radiance computations used here for the ERA-40 short-range forecasts have been performed directly within the ERA-40 processing and are part of the archive. This dataset is used in section 4 and is simply referred to as 'ERA-40' in that section.

In order to process other data, like the analyses, longer forecast ranges or ERA-15, as is done in sections 5 and 6, a simpler high cloud detection is defined. The method is based on the idea that the HIRS is more sensitive to changes in the cloud ice contents in the FOV than to changes in its horizontal spread (see Fig. 10 of Chevallier et al. 2001). A high cloud is diagnosed when the the mean cloud ice column in the model grid box above 440 *hPa* exceeds 2.10^{-5} $kg.m^{-2}$ within 30° latitude from the Equator and 5.10^{-5} $kg.m^{-2}$ elsewhere. The mean cloud ice contents in the model grid box are computed by dividing the layer cloud ice contents in the clouds by the layer cloud covers. Global model fields are processed at the temporal resolution of the archive (every six hours for ERA-15 and ERA-40 analyses, every twelve hours for medium and long ERA-40 ranges, except where indicated), without any reference to the observation date and location. This simplification would not be apropriate over land.

The quality of the high cloud occurrence based on this empirical cloud detection is evaluated in section 5.

4 Comparison between ERA-40, HIRS and ISCCP

The high clouds in the ERA-40 short-range forecasts are compared to HIRS retrievals and to the ISCCP climatology. It is obvious that the HIRS-like post-processing of the model data described in the previous section is intended to make it close to HIRS rather than to ISCCP.

4.1 Mean annual cycle

Figures 4 and 5 present the mean high cloud frequencies for January, April, July and October between July 1983 and September 2001. HIRS and ERA-40 frequencies are larger than those shown by Chevallier et al. (2001) due to a revision of the implementation of the CO_2-slicing algorithm. The three datasets grossly agree with each other for the broad patterns of the mid-latitude storm tracks and of the intertropical, South Pacific, South Atlantic and South Indian convergence zones. One example is the double structure of the ITCZ which exists during some boreal springs in the eastern Pacific (e.g. Hubert et al. 1969) and that appears in the three April monthly means. Despite the particularly good agreement between HIRS and ISCCP for the horizontal patterns, occurrences are smaller in ISCCP due to different sensitivities to thin cirrus (Jin et al. 1996). One may notice a large circular pattern in the western Indian ocean for ISCCP. It is located about the border of the disk of the Meteosat satellite stationed close to zero degree longitude and may indicate some remaining calibration issue for this database as well.

Consistent with previous results (Chevallier et al. 2001), ERA-40's ITCZ appears too static and frequencies seem to be underestimated in the mid-latitudes. One may note as well that the seasonal cycle around the Tropic of Cancer is not adequately represented in the western Pacific, with too high values north of the ITCZ in April, and an excessive northern ITCZ extent in July and October. Lastly, the northern Atlantic storm track pattern in July and October reproduces neither ISCCP nor HIRS along the east coast of America.

4.2 Interannual anomalies

In the context of a changing climate, much focus has been put on trend estimation (e.g., IPCC 2001). Interannual anomalies from ERA-40, HIRS and ISCCP are compared in this section. They are computed for each dataset by removing the mean annual cycles previously shown in Fig. 4 and 5.

Figure 6 presents the mean cloud frequency anomalies for all clouds and for high clouds only over the 60°S-60°N oceans. Time series have been smoothed with a two-side exponentially weighted average to ease the

visualisation. The ISCCP trend for all clouds (Fig. 6b) is very similar to the ISCCP global (land and ocean) trend shown in Fig. 6a of Rossow and Schiffer (1999), with an increase before 1987 and an overall decrease afterwards. In contrast, the HIRS-based cloud detection seems to be dominated by the 1982-83, 1991-92 and 1997-98 El Niño episodes for which years significant increases occur and an overall 23-yr trend can hardly be estimated. No significant interannual variations can be seen in ERA-40, likely due to excessive low cloud occurrence (Chevallier et al. 2001).

A slightly better agreement between the three datasets exists for high cloud anomalies, but differences still make it difficult to conclude on the actual trends of the atmosphere (Fig. 6a). The largest disagreement between HIRS and ISCCP concerns the 1991-92 period and may be attributed to the impact of volcanic aerosols from the eruption of Mt. Pinatubo, that ISCCP is known not to have properly handled (Luo et al. 2002). The reason for other disagreements, like in 1986-88, in 1990 or at the end of the record, is not obvious but it may be interesting to study possible relationships between them and the availability of individual satellite instruments for HIRS and ISCCP. ERA-40 differs from HIRS in the 1980s, but reproduces its main patterns from 1991 onwards, even though the final increase occurs one year too early.

For further comparison of the high clouds trends, the globe ocean surface is divided into the ten regions shown in Table 1. The difference between ISCCP and HIRS, and between ERA-40 and HIRS are displayed in Fig. 7 with the polar representation proposed by Taylor (2001). The radial axis indicates the standard deviation of one the datasets normalised with that of the other one, while the angular axis indicates the correlation between the two datasets concerned. HIRS is the reference in the two diagrams of Fig. 7 and consequently appears on the graphs at location (1,1), i.e. with a unity normalised standard deviation and a unity correlation. The differences of the other dataset (ISCCP in Fig. 7a and ERA-40 in Fig. 7b) with the reference is visualised by letters symbolysing the ten maritime regions studied. By construction, the distance between those points on the graph and the reference at location (1,1) is a normalised standard deviation of the differences between the two datasets (Taylor 2001).

Figure 7a shows a large spread of the differences between ISCCP and HIRS. Correlations are 0.6 for the Tropical regions from the Indian to the East Pacific only, regions that are dominated by the Indian monsoon circulation and the El Niño southern oscillation (ENSO). For other regions, the two datasets do not describe the same variations of the atmosphere.

As detailed before, ERA-40 has been post-processed to reproduce the HIRS climatology and indeed the correlations between ERA-40 and HIRS, with values above 0.5 for all regions, are noticeably positive. The correlations are even larger (above 0.6) when the comparison is extended to the 23 years of the HIRS database (not shown). The ERA-40 anomaly amplitude is also close to HIRS with normalised standard deviations between 0.8 and 1.2, but usually smaller than one, as can be expected from the underestimation of high cloud occurrence in the extratropics.

5 Evaluation of ERA-15

As discussed in section 3.4, a simple threshold method is used to post-process ERA-15, rather than the elaborate HIRS simulator. The impact of this simplification can be seen in Fig. 8c, 8d, and 9 for ERA-40. The high cloud seasonal cycle (Fig. 8c and 8d, to be compared with 4c and 5c respectively) is marginally affected. The anomaly correlations and the normalised standard deviations are slightly degraded, by up to 0.1 for both quantities (Fig. 9).

The seasonal cycle of high clouds appears to have been dramatically improved between ERA-15 and ERA-40 (Fig. 8), with increased contrast between the regions of ascent and descent. A side detrimental effect can be

seen around the Tropic of Cancer in the western Pacific, where the ERA-40 ITCZ erroneously extends more northward than in ERA-15 in summer.

The anomalies displayed in Fig. 10 also show an improved realism from ERA-15 to ERA-40 in all regions but one, with correlations about 0.1 higher in ERA-40 while the normalised standard deviations are stable. The exception is the Tropical West Pacific area where the ERA-40 signal amplitude is 0.2 further away from the reference, compared to ERA-15.

6 ERA-40 before HIRS

So far, this study has only focused on the evaluation of the ECMWF re-analyses for the HIRS period. It has therefore covered the full ERA-15 record but only half of the ERA-40 archive, which starts in 1957. It was found in section 3.3 that the VTPR observations cannot serve yet as a reference, as was initially intended. It is most likely that the calibration issues that were underlined actually affected the quality of ERA-40 in the mid-1970s. For the late 1950s, the 1960s and the early 1970s, only conventional observations exist and they constrain the analysis mainly in the northern hemisphere. The lack of validation data parallels the lack of observations to be assimilated. The present study attempts to evaluate the pre-HIRS period of ERA-40, on the basis of the above results for the HIRS period. As in the previous section, clouds are detected in ERA-40 with the simple threshold method defined in section 3.4.

The trends for the whole ERA-40 analysis archive are displayed in Fig. 11 and 12. Several interesting features can be noticed. First, the anomaly variability seems to be much reduced before the HIRS observations are available. In particular, the impact of ENSO hardly appears in the Tropical East Pacific before the 1980s. SST anomalies associated with ENSO events have been larger in the 1980s and 1990s (e.g., Trenberth and Hoar 1997), but the amplitude decrease of the ERA-40 high cloud anomalies for the earlier decades compared to the later ones seems to be much overestimated. Other likely artifacts of the ERA-40 record can be noticed in relation to VTPR. The introduction of NOAA-2 data is accompanied by an increase of high cloudiness in most of the Tropics and in the northern Pacific. The erroneous bias-correction for NOAA-3, mentioned in section 3.3, likely generated the cloudiness decrease in 1975-76 observed in the southern mid-latitudes. Lastly, significant variations in the number of available radiosondes before mid-1958 may explain the anomaly drop in ERA-40 during that period.

A complementary assessment of the pre-satellite period of ERA-40 is provided by the 45-yr climate simulation that was run for the ERA-40 period with the same forecast model and at the same spatial resolution. That simulation was solely forced by the SST and sea ice fields and represents the extreme case where no observation is fed to the analysis system. Figure 13 illustrates the seasonal cycle of the run with the mean high cloud frequencies for January and July between July 1983 and September 2001. That period is chosen to allow the comparison with the HIRS observations of Fig. 4 and 5. Two main features distinguish the high clouds in the climate simulation from the ERA-40 analyses (Fig. 4-5 and 8). The first one is the increase of occurrence in the extra-tropics, which makes them closer to the observations. The behaviour of the convergence zones in the Indian ocean and in the western Pacific is the second one. The model ITCZ systematically splits into two branches in the Indian ocean. and the South Pacific convergence zone (SPCZ) separates from the ITCZ too much westward. Those results actually corroborate known weaknesses of the forecast model (e.g. Jung and Tompkins 2003). In consequence, the climate simulation anomalies, displayed in Fig. 14, do not correlate with the observations in any of the ten maritime regions considered.

The imbalance between the analyses and the model physics is noticeable on short-range forecasts as well. For instance Fig. 15 shows that systematic differences exist between the 36-hour forecasts and the analyses: the frequencies of high clouds diminish in the ITCZ away from the analysis, the ITCZ shifts northward in the

Atlantic and Pacific oceans in July, the SPCZ shifts southward in January and the ITCZ organisation varies in the Indian ocean. It is worth noting that the reduction of high cloud occurence in the ITCZ is consistent with the known loss of specific humidity by the forecast model during the first hours and days of the integrations, through excessive convective precipitation (Jung and Tompkins 2003).

7 Conclusions

The representation of clouds in general, and high ones in particular, has proven to be a challenge for modellers. Furthermore, clouds are not the main focus of ERA-15 and ERA-40, since they are not directly analysed. Temperature for instance is a far more reliable variable in both re-analyses. However, it is of interest to see how re-analyses perform for less emblematic parameters in order to define their range of possible applications. This study attempted to evaluate ERA-15 and ERA-40 high cloud climatologies over ocean on the basis of both VTPR and HIRS cloud retrievals.

The CO_2-slicing method of Wylie et al. (1994) has been used to retrieve cloud top pressures and cloud emissivities from VTPR and HIRS. The constitution of the retrieval dataset already gave some information about the quality of ERA-40 since it used the ERA-40 radiance bias-correction. It was shown that the bias-correction successfully calibrated the data from many of the instruments uniformly. However, instruments on-board five of the 15 platforms were not calibrated with the same accuracy. The impact on ERA-40 is much larger during the mid-1970s when only one weather satellite is usually available. In addition, it was noticed that some of the satellite data had not been assimilated. Some data were left out because the system could only handle two NOAA satellites at once. Other data were passively monitored to set up the radiance bias-correction and the corresponding periods have not be re-run. These issues are currently being addressed and improvements should be made for future ECMWF re-analyses.

The CO_2-slicing algorithm has been adapted to VTPR. The impact of different channels and FOVs on the cloud retrievals results in VTPR cloud occurrences 5 to 10% higher than those from HIRS. Merging the VTPR and HIRS records is consequently challenging. Similar difficulties will be met to make the AIRS or the forthcoming Infrared Atmospheric Sounding Interferometer (IASI) observations compatible with the HIRS or even with the VTPR. Ideally, the instrument spectral and horizontal resolutions should be degraded to fit the lower quality one (i.e. VTPR) in order to constitute a homogeneous climatology suitable for the study of atmospheric trends.

Based on the HIRS record, a new 23-yr climatology of high cloud frequencies has been gathered. It should ultimately be compared to the similar Wisconsin University archive that is being re-processed. Unsurprisingly it shows different trends than ISCCP, which is less driven by thin cirrus. The discrepancy illustrates the difficulty of assessing climate changes from remote-sensed observations. It may be noted that this new 23-yr climatology does not indicate any change of cirrus occurrence in the main air-traffic flight corridors. The reason for disagreement with previous results based on surface observations (Boucher 1999) could be a consequence of the lower resolution of the satellite data.

The ERA-15 and ERA-40 analyses and short-range forecasts have been compared to the HIRS climatology. Consistent with the preliminary study of Chevallier et al. (2001), the ERA-40 ITCZ is too static and the cloud ice water seems underestimated in the extra-tropics. It was also found that the seasonal variations around the Tropic of Cancer are not adequately represented in the western Pacific and Atlantic oceans for ERA-40. Despite these weaknesses, ERA-40 dramatically improves on ERA-15 for the realism of the seasonal and interannual variations in high clouds. More than 60% of the observed anomalies during the January 1979 - February 2002 period in large oceanic basins are captured by the latest re-analysis.

The quality of high clouds from ERA-40 for the 1960s and the 1970s has been qualitatively assessed. The real-

ism of the analyses in the areas with sparse observations or even none, like the southern oceans or the Tropical Pacific in the 1960s appears to be poor. In those regions, the analysis system is mainly driven by the model physics, which was primarily developed for forecasting purposes rather than for long climate runs. In particular, the model radiative budget at the top of the atmosphere is notably poor (Chevallier and Morcrette 2000), despite a good simulation of its clear-sky component (Allan and Ringer 2003). Moreover, the inadequate calibration of some of the VTPR observations does not make ERA-40 much more reliable in the mid-1970s in those areas where conventional observations are sparse. To summarise, it is unlikely that the ERA-40 interannual variations in most parts of the world can be trusted before 1977 or even 1979. The imbalance between the analyses and the model physics was also noted for short-range forecasts for the 1980s and 1990s.

This study focussed on time scales longer than the month and at 2.5° horizontal resolution. We have also evaluated the model radiances for many extra-tropical cyclones and found no indication of systematic errors, apart from the above-mentioned underestimation of the cloud ice. However the time-space sampling of the polar-orbiters makes it difficult to draw firm conclusions about the quality of synoptic weather systems in ERA-40. The use of geostationary data for validation would be more appropriate. Readers are referred to Chevallier and Kelly (2002) for an evaluation of the ECMWF operational forecasting system with Meteosat radiances. ERA-40 is expected to compare less favourably due to reduced horizontal resolution (125 vs. 40 *km*).

ECMWF will work towards an extensive new re-analysis which could begin in 2008 or beyond. Already, major changes to the forecasting system are being made to improve the representation of the hydrological cycle (Andersson et al. 2003a, 2003b). In particular, the assimilation of satellite radiances affected by high clouds is being prepared (Chevallier et al. 2003), which should improve the quality of the upper tropospheric humidity in the cloud systems. The next re-analysis is expected to significantly benefit from these developments.

Acknowledgements

The Satellite Application Facility on Numerical Weather prediction which is co-sponsored by Eumetsat supported part of this work. The ERA-40 project involved many people at ECMWF and in partner institutes and was partially funded by the European Commission through contract EVK2- CT-1999-00027. The authors gratefully acknowledge the fruitful interaction with D. P. Wylie and P. Menzel at Wisconsin University.

References

Allan, R. P. and Ringer, M. A., 2003: Inconsistencies between satellite estimates of longwave cloud forcing and dynamical fields from reanalyses. *Geophys. Res. Lett.*, **30(9)**, 1491, doi:10.1029/2003GL017019

Andersson, E., P. Bauer, A. Beljaars, F. Chevallier, E. Hólm, M. Janisková, P. Kållberg, G. Kelly, P. Lopez, A. McNally, E. Moreau, A. Simmons and J.-N. Thépaut, 2003a: Assimilation and modelling of the hydrological cycle. *Bull. Amer. Meteo. Soc, submitted.*

Andersson, E., A. Beljaars, J. Bidlot, M. Miller, A. Simmons and J.-N. Thépaut, 2003b: A major new cycle of the IFS: Cycle 25r4. *ECMWF Newsletter*, **97**, 12-20.

Boucher, O., 1999: Air traffic may increase cirrus cloudiness, *Nature*, **397**, 30-31.

Brest, C. L., W. B. Rossow, and M. D. Roiter, 1997: Update of radiance calibrations for ISCCP. *J. Atmos. Oceanic Technol.*, **14**, 1091-1109.

Chahine, M. T., 1974: Remote sounding of cloudy atmospheres. I. The single cloud layer. *J. Atmos. Sci.*, **31**, 233-243.

Chevallier, F., and J.-J. Morcrette, 2000: Comparison of model fluxes with surface and top-of-the-atmosphere observations. *Mon. Wea. Rev.*, **128**, 3839-3852.

Chevallier, F., P. Bauer, G. Kelly, C. Jakob, and T. McNally 2001: Model clouds over oceans as seen from space: comparison with HIRS/2 and MSU radiances. *J. Climate*, **14**, *4216-4229.*

Chevallier, F., and G. Kelly, 2002 : Model clouds as seen from space: comparison with geostationary imagery in the 11μm window channel. *Mon. Wea. Rev.*, **130**, *712-722.*

Chevallier, F., P. Lopez, A. M. Tompkins, M. Janisková and E. Moreau, 2003: The capability of 4D-Var systems to assimilate cloud-affected satellite infrared radiances. *Q. J. R. Meteor. Soc., in press*.

Eyre, J. R., 1991: A fast radiative transfer model for satellite sounding systems. *ECMWF Technical Memorandum No. 176*, 28 pp.

Gibson, J. K., P. Kållberg, S. Uppala, A. Hernandez, A. Nomura, and E. Serrano, 1997: ECMWF Re-analysis. 1. ERA description. ECMWF Project Report Series, 72 pp.

Goodrum, G., K. B. Kidwell, and W. Winston, 2000: NOAA KLM User's Guide. NOAA, NESDIS, NCDC, Climate Services Division, Satellite Services Branch. September 2000 revision.

Available online at: http://www2.ncdc.noaa.gov/docs/klm/index.htm

Harris, B. A., and G. Kelly, 2001: A Satellite Radiance Bias Correction Scheme for Radiance Assimiliation. *Q. J. Roy. Meteor. Soc.*, **127**, 1453-1468.

Hernandez, A., R. W. Saunders, A. P. McNally, G. Kelly, S. Uppala and P. Kållberg, 2000: The use of TOVS/ATOVS data in ERA-40. *Proc. of the Second WCRP International Conference on Reanalyses, nr. Reading, U.K., 23-27 August 1999*, WCRP-109, WMO/TD-No. 985, 69-72.

Hubert, L. F., A. F. Krueger, and J. S. Winston, 1969: The double intertropical convergence zone–Fact or fiction? *J. Atmos. Sci.*, 26, 771-773.

IPCC, 2001: Climate Change 2001: The Scientific Basis. Cambridge University Press, UK, 881 pp.

Jakob, C., 1999: Cloud cover in the ECMWF reanalysis. *J. Climate*, **12**, 947-959.

Jin, Y, W. B. Rossow, and D. P. Wylie, 1996: Comparison of the climatologies of high-level clouds from HIRS and ISCCP. *J. Climate*, **9**, 2850-2879.

Jung, T. and A. Tompkins, 2003: Systematic errors in the ECMWF forecasting system. *ECMWF Technical Memorandum No. 422*, 72 pp.

Kidwell, K. B., 1998: NOAA polar orbiter data user's guide. Technical report. NOAA, NESDIS, NCDC, Climate Services Division, Satellite Services Branch, November 1998 revision.

Available online at: http://www2.ncdc.noaa.gov/docs/podug/index.htm

Liao, X., W. B. Rossow, and D. Rind 1995. Comparison between SAGE II and ISCCP high-level clouds: 1. Global and zonal mean cloud amounts. *J. Geophys. Res.*, **100**, 1121-1135.

Li, X., S. Uppala, J.K. Gibson, R. Saunders, 2000: The use of VTPR-1c Data in ERA-40, Part I: preprocessing. *Proc. of the Second WCRP International Conference on Reanalyses, nr. Reading, U.K., 23-27 August 1999*, WCRP-109, WMO/TD-No. 985, 73-76.

Luo, Z., W. B. Rossow, T. Inoue, and C. J. Stubenrauch 2002. Did the eruption of the Mt. Pinatubo volcano affect cirrus properties? *J. Climate*, **15**, 2806-2820.

McMillin, L. M., D. Q. Wark, J. M. Siomkajlo, P. G. Abel, A. Werbowetzki, L. A. Lauritson, J. A. Pritchard, D. S. Crosby, H. M. Woolf, R. C. Luebbe, M. P. Weinreb, H. E., Fleming, F. E. Bittner, and C. M. Hayden, 1973: Satellite infrared soundings from NOAA Spacecraft. U.S. Department of Commerce, NOAA Technical Report NESS 65, 112 pp.

Morcrette, J.-J., E. J. Mlawer, M. J. Iacono, and S. A. Clough, 2001: Impact of the radiation–transfer scheme RRTM in the ECMWF forecasting system. *ECMWF Newsletter*, **91**, 2-9.

Price, J.C., 1991: Timing of NOAA afternoon passes. *Int. J. Remote Sensing*, **12**, 193-198.

Rossow, W. B. , and R. A. Schiffer, 1999: Advances in understanding clouds from ISCCP. *Bull. Amer. Meteor. Soc.*, **80**, 2261-2287.

Saunders, R., M. Matricardi, and P. Brunel, 1999: An improved fast radiative transfer model for assimilation of satellite radiance observations. *Quart. J. Roy. Meteor. Soc.*, **125**, 1407-1425.

Scott, N. A., A. Chédin, R. Armante, J. Francis, C. Stubenrauch, J.-P. Chaboureau, F. Chevallier, C. Claud, and F. Chéruy, 1999: Characteristics of the TOVS Pathfinder Path-B database. *Bull. Amer. Meteo. Soc, 80, 2679-2702.*

Simmons, A. J., and J. K. Gibson (Eds), 2000: The ERA-40 project plan. *ERA-40 Project Report Series No. 1*, 62 pp.

Simmons, A. J., 2001: Development of the ERA-40 data assimilation system. *ERA-40 Project Report Series No. 3*, 11-30.

Simmons, A. J., and A. Hollingsworth, 2002: Some aspects of the improvement of skill of numerical weather prediction. *Quart. J. Roy. Meteor. Soc.*, **128**, 647-677.

Smith, W. L. and Woolf, H. M. and Hayden, C. M. and Wark, D. Q. and McMillin, L. M., 1979: The TIROS-N operational vertical sounder. *Bull. Amer. Meteor.*, **60**, 1177-1187.

Susskind, J., P. Piraino, L. Rokke, L. Iredell, and A. Mehta., 1997: Characteristics of the TOVS Pathfinder Path A Dataset. *Bull. Amer. Meteor. Soc.*, **78**, 1449-1472.

Taylor, K. E., 2001: Summarizing multiple aspects of model performance in a single diagram. *J. Geophys. Res.*, **106**, 7183-7192.

Tiedtke, M., 1993: Representation of clouds in large-scale models. *Mon. Wea. rev.*, **121**, 3040-3061.

Trenberth, K. E. and T. J. Hoar, 1997: El Niño and climate change. *Geophys. Res. Lett.*, **24**, 3057-3060.

Wylie, D. P., W. P. Menzel, H. M. Woolf, and K. I. Strabala, 1994: Four years of global cirrus cloud statistics using HIRS. *J. Climate*, **7**, 1972-1986.

Wylie, D. P., and P.-H. Wang, 1997: Comparison of cloud frequency data from the High-resolution Infrared

Radiometer Sounder and the Stratospheric Aerosol and Gas Experiment II. *J. Geophys. Res.*, **102**, 29,893-29,900.

Wylie, D. P., and W. P. Menzel, 1999: Eight years of high cloud statistics using HIRS. *J. Climate*, **12**, 170-184.

Maritime region	Boundaries		Symbol
Tropical Atlantic	20°S-20°N	60°W-20°E	b
Tropical Indian	20°S-20°N	50°E-100°E	c
Indonesia	20°S-20°N	100°E-140°E	d
Tropical West Pacific	20°S-20°N	140°E-180°E	e
Tropical East Pacific	20°S-20°N	180°W-100°W	h
Northern Atlantic	20°N-60°N	70°W-0°	k
Northern Pacific	30°N-60°N	160°E-140°E	m
Southern Atlantic	60°S-30°S	70°W-20°E	p
Southern Indian	60°S-30°S	20°E-140°E	s
Southern Pacific	60°S-30°S	140°E-170°E	v

Table 1: Definition of the maritime regions used.

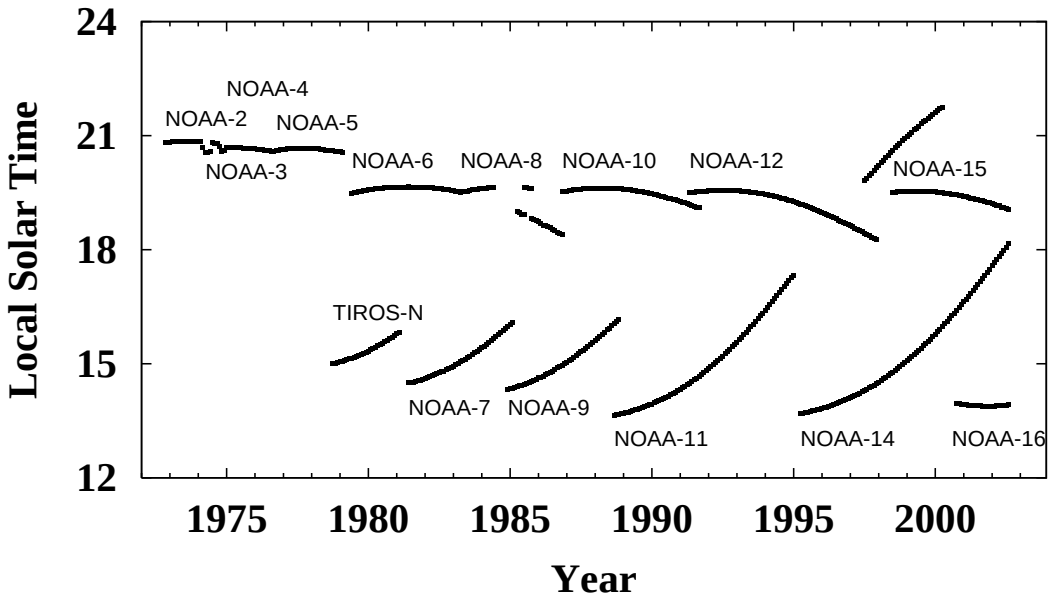

Figure 1: Local solar time of the ascending node (northbound equator crossing) of the NOAA satellite series. Satellites launched before 1978 carry the VTPR instrument. HIRS is on-board the platforms from TIROS-N onwards.

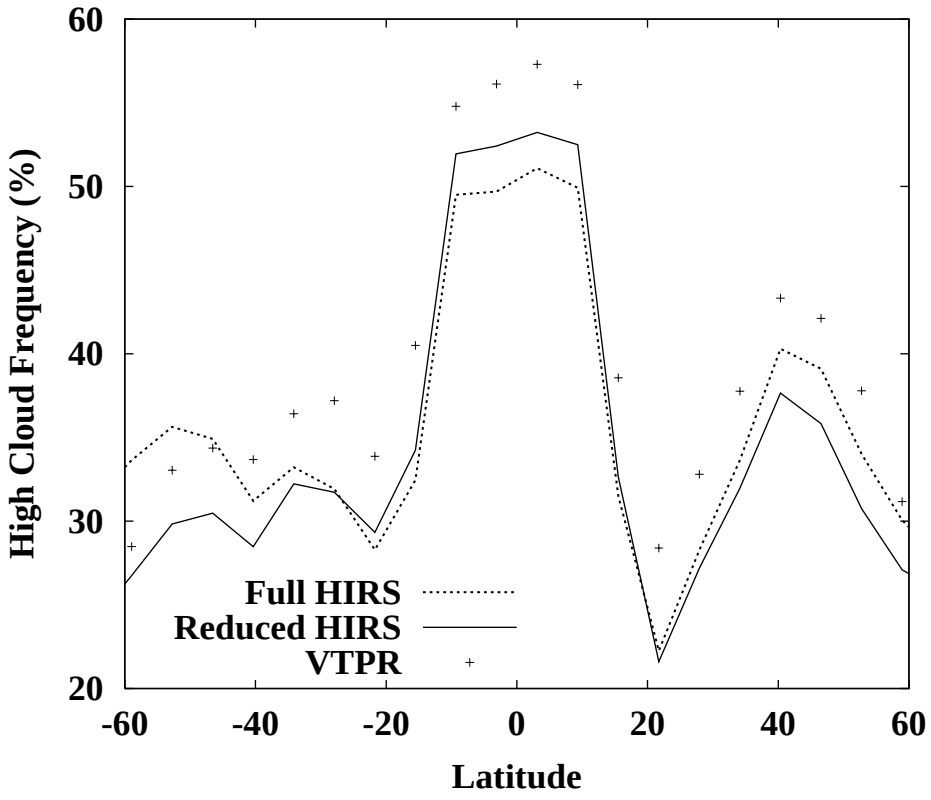

*Figure 2: Frequency of high cloud in the zonal mean for December 1978 over open oceans. The retrieval is made with five HIRS channels (*Full HIRS*), with three HIRS channels (*Reduced HIRS*) or with VTPR.*

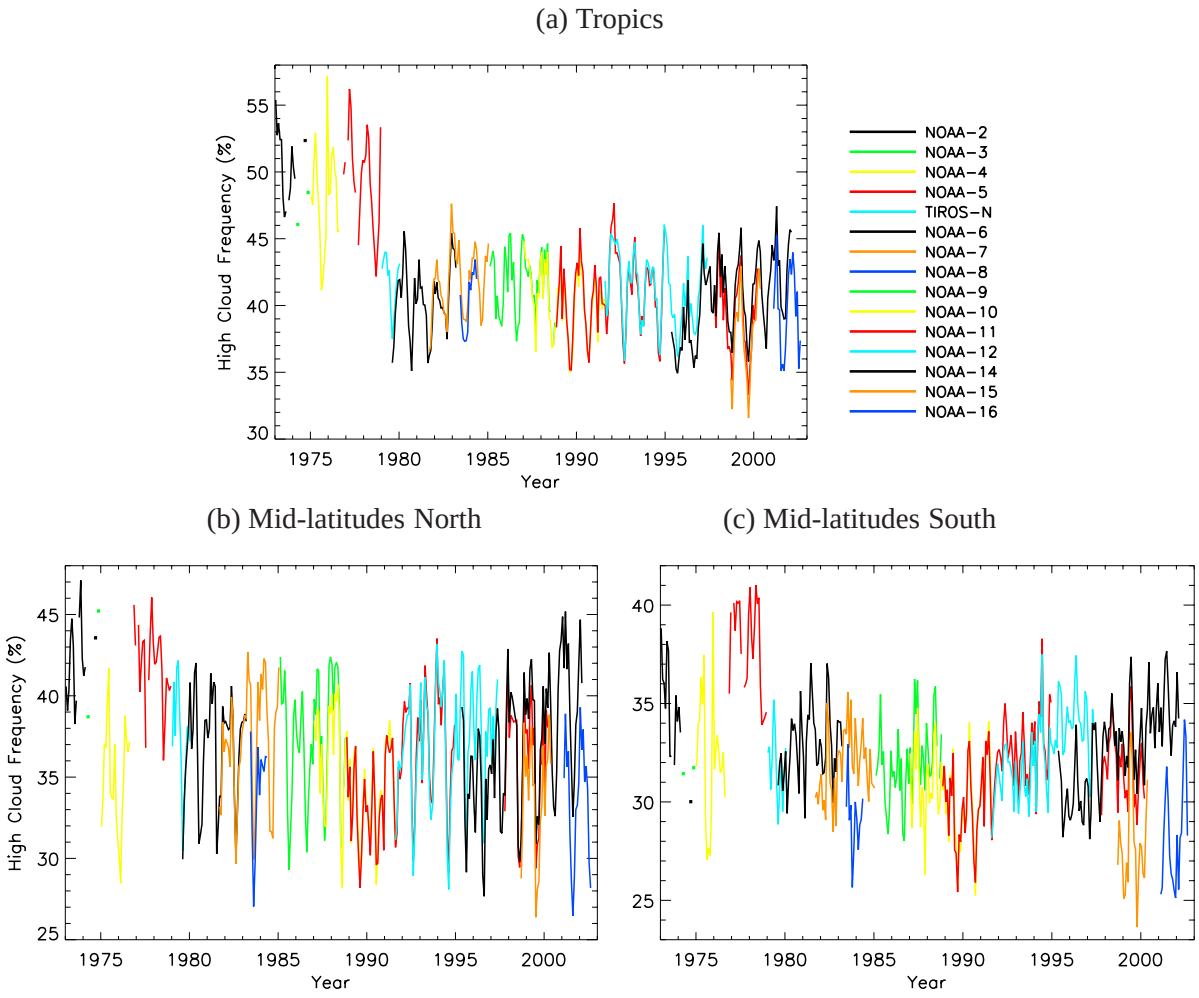

Figure 3: Frequency of high clouds in the tropics (15°S-15°N), in the northern mid-latitudes (30°N-50°N) and in the southern mid-latitudes (30°S-50°S). The distinction is made between the estimation from each individual satellite. Statistics for a particular platform and a particular month were computed when data are regularly spread in both time and space troughout the month for that platform. Data of suspicious quality, as indicated by the ERA-40 'blacklist' files, were removed.

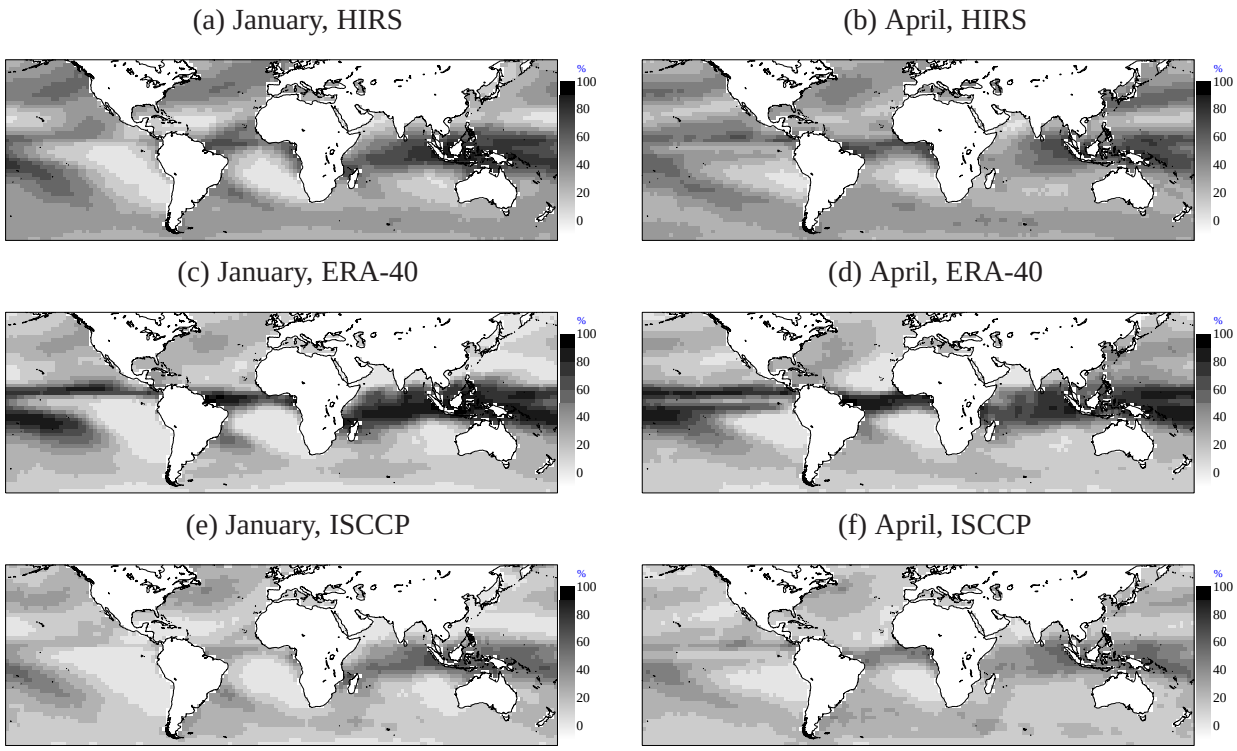

Figure 4: Mean frequency of high clouds from HIRS, ERA-40 and ISCCP for January and April between July 1983 and September 2001.

(a) July, HIRS

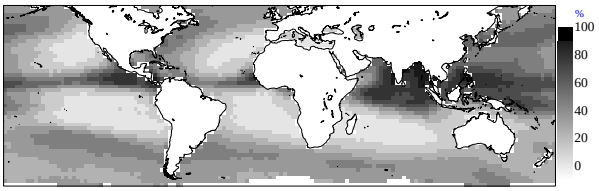

(b) October, HIRS

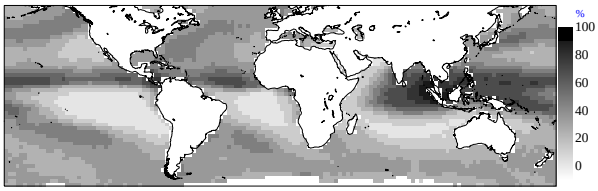

(c) July, ERA-40

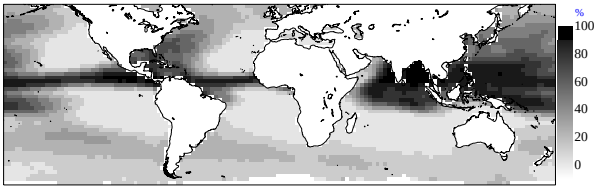

(d) October, ERA-40

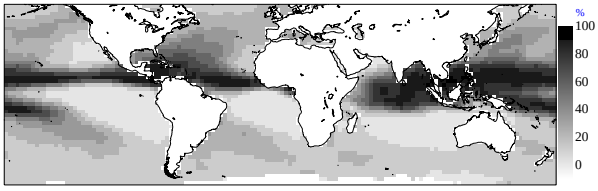

(e) July, ISCCP

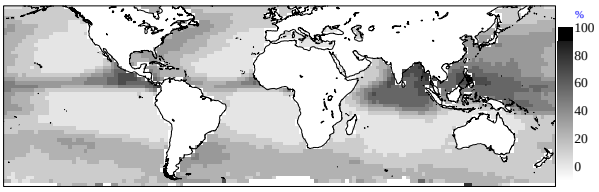

(f) October, ISCCP

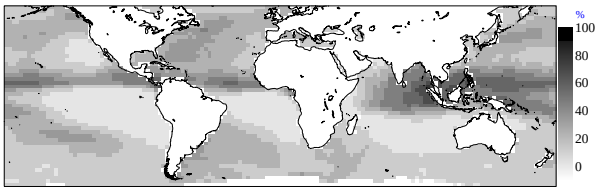

Figure 5: Same as Fig. 4 for July and October.

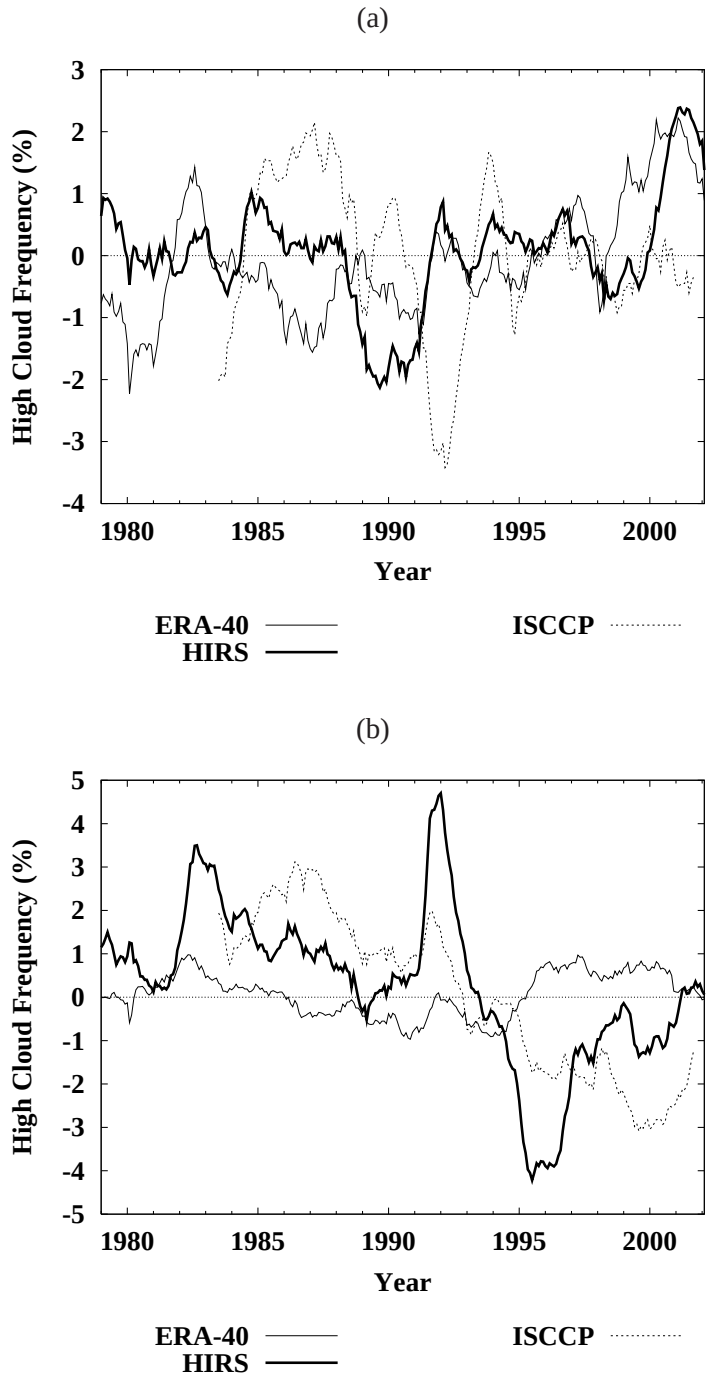

Figure 6: Mean high (top) and total (bottom) cloud frequency anomalies over $60\,°S - 60°N$ *oceans from ERA-40, HIRS and ISCCP. Monthly anomalies are defined for each dataset with respect to its July 1983 - September 2001 climatology. Curves have been smoothed with a two-side exponentially weighted average.*

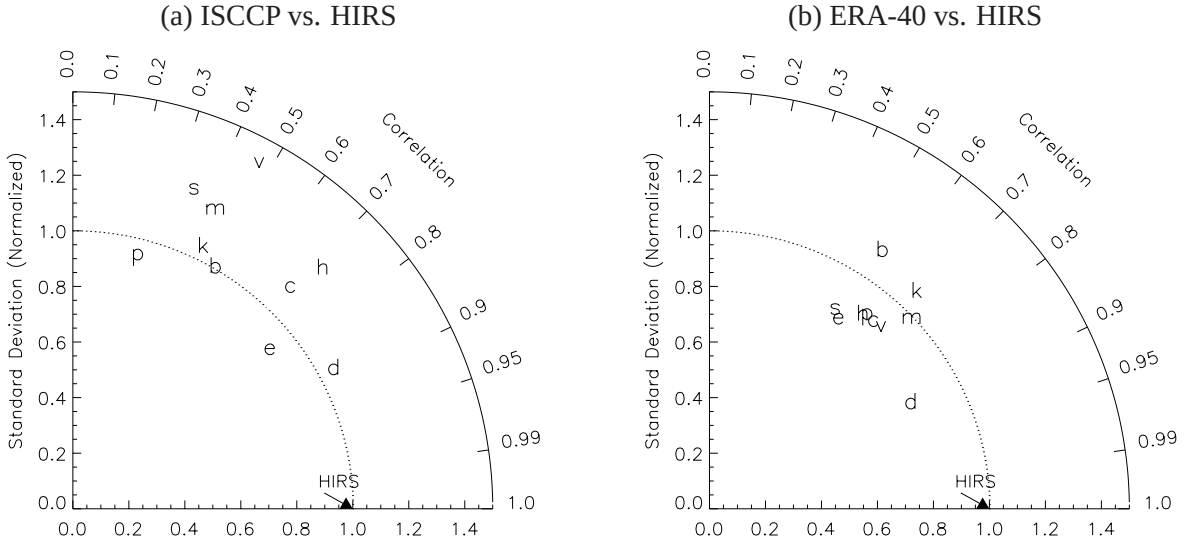

Figure 7: Polar representation of normalised standard deviations (radius) vs. correlations (angle) between the high cloud frequency anomalies from HIRS and from ISCCP (left) or from ERA-40 (right). Monthly anomalies are defined for each dataset with respect to its July 1983 - September 2001 climatology. Statistics are computed for the ten maritime regions of Table 1.

(a) January, ERA-15

(b) July, ERA-15

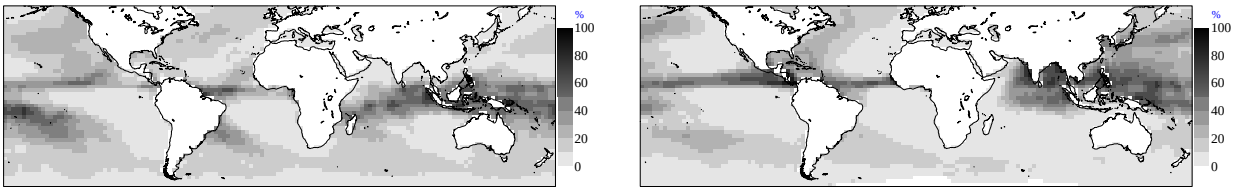

(c) January, ERA-40

(d) July, ERA-40

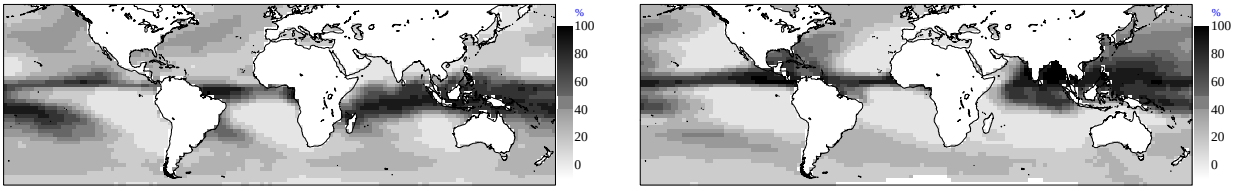

Figure 8: Mean frequency of high clouds from ERA-15 and ERA-40 analyses for January and July between January 1979 and December 1993. For both ERA-15 and ERA-40, high clouds are detected from the cloud ice profiles.

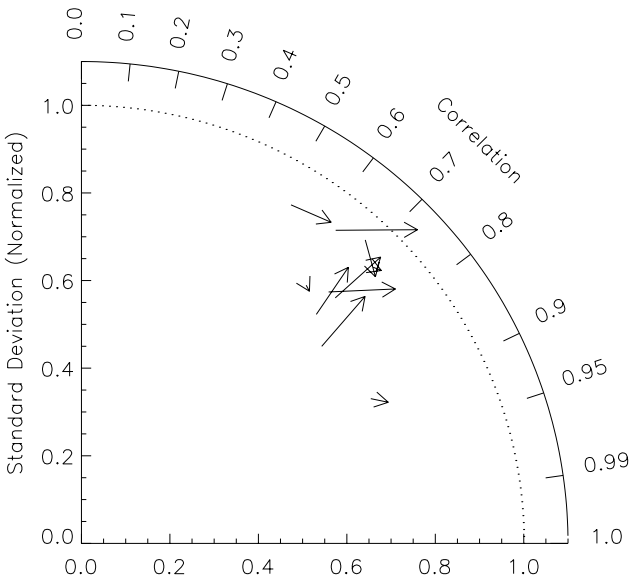

Figure 9: Polar representation of normalised standard deviations (radius) vs. correlations (angle) between the high cloud frequency anomalies from HIRS and ERA-40 using the analysis cloud ice profiles (tail of the arrows) or the radiance computation (head of the arrows). Monthly anomalies are defined for each dataset with respect to its January 1979 - December 1993 climatology. Statistics are computed for the ten maritime regions of Table 1, but for clarity the arrows are not labelled.

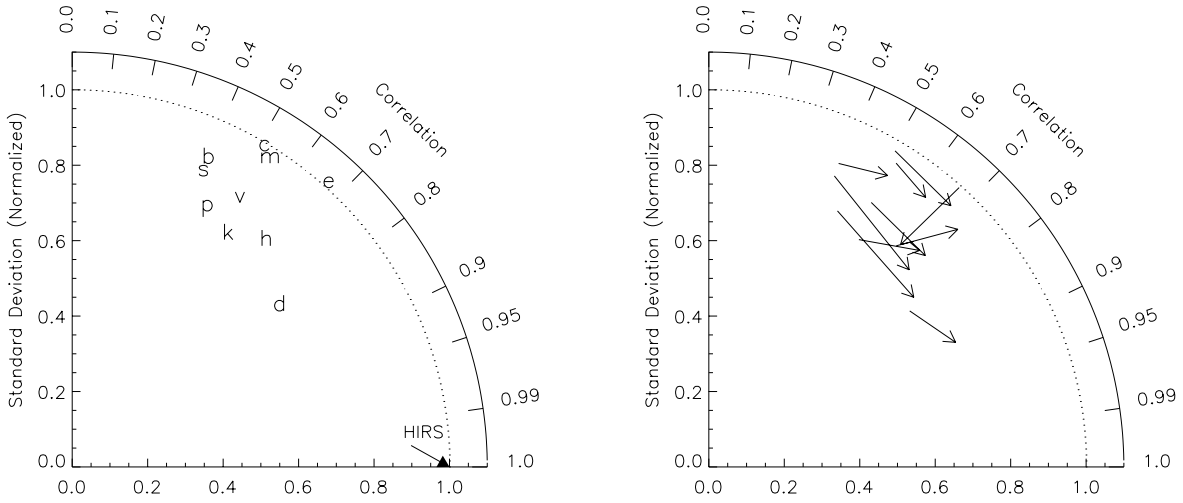

Figure 10: Polar representation of normalised standard deviations (radius) vs. correlations (angle) between the high cloud frequency anomalies from HIRS and ERA-15 (left figure and tail of the arrows in the right figure) or ERA-40 (head of the arrows in the right figure). For both ERA-15 and ERA-40, high clouds are detected from the cloud ice profiles. Monthly anomalies are defined for each dataset with respect to its January 1979 - December 1993 climatology. Statistics are computed for the ten maritime regions of Table 1.

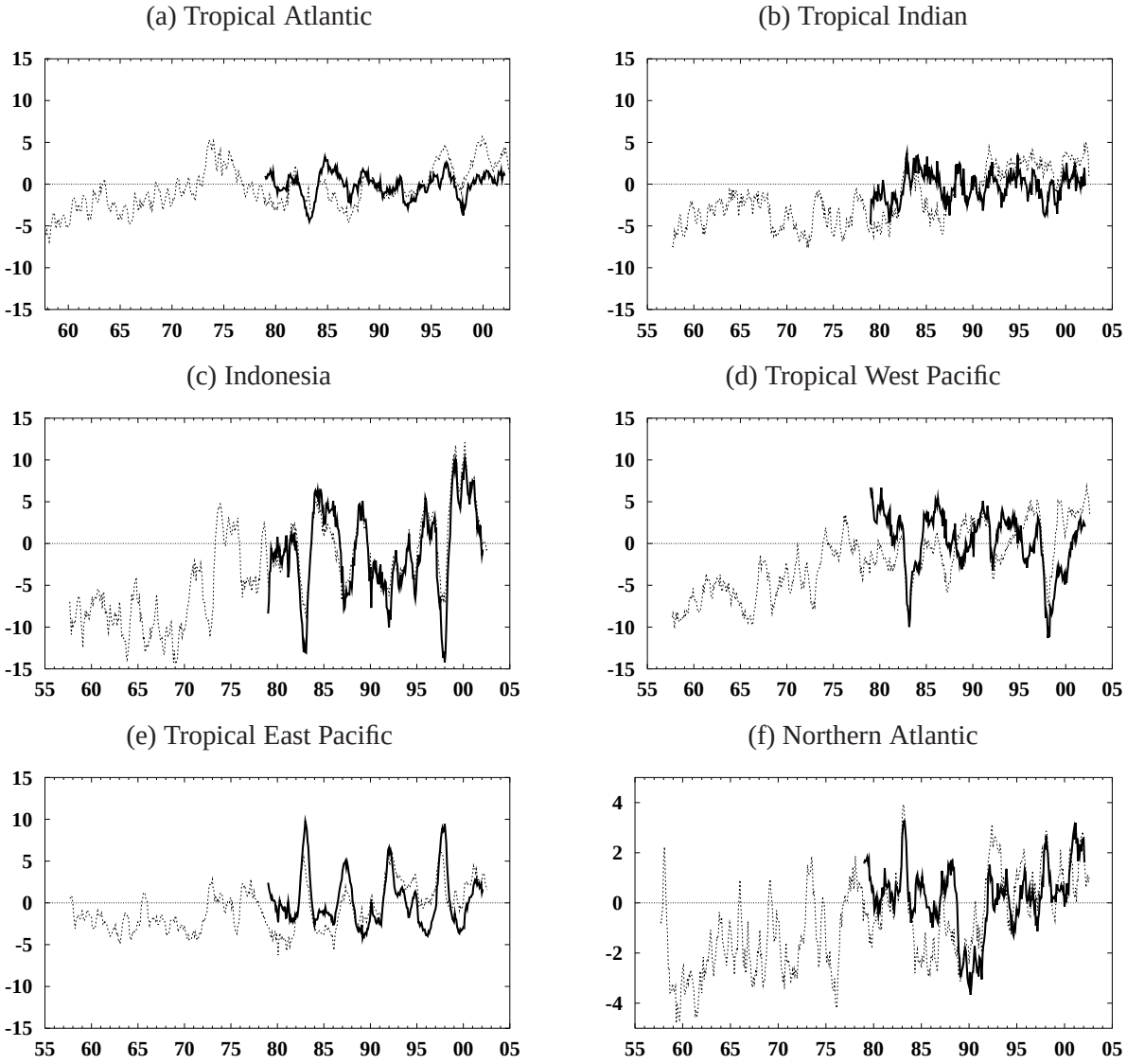

Figure 11: Mean frequency of high cloud anomalies from ERA-40 analyses (dotted lines) and from HIRS (thick lines) for the first six maritime regions of Table 1. Curves have been smoothed with a two-side exponentially weighted average. Note that the ordinate scale is smaller in the Tropics. Monthly anomalies are defined for each dataset with respect to its January 1979 - February 2002 climatology. High clouds are detected in the ERA-40 analyses from the cloud ice profiles.

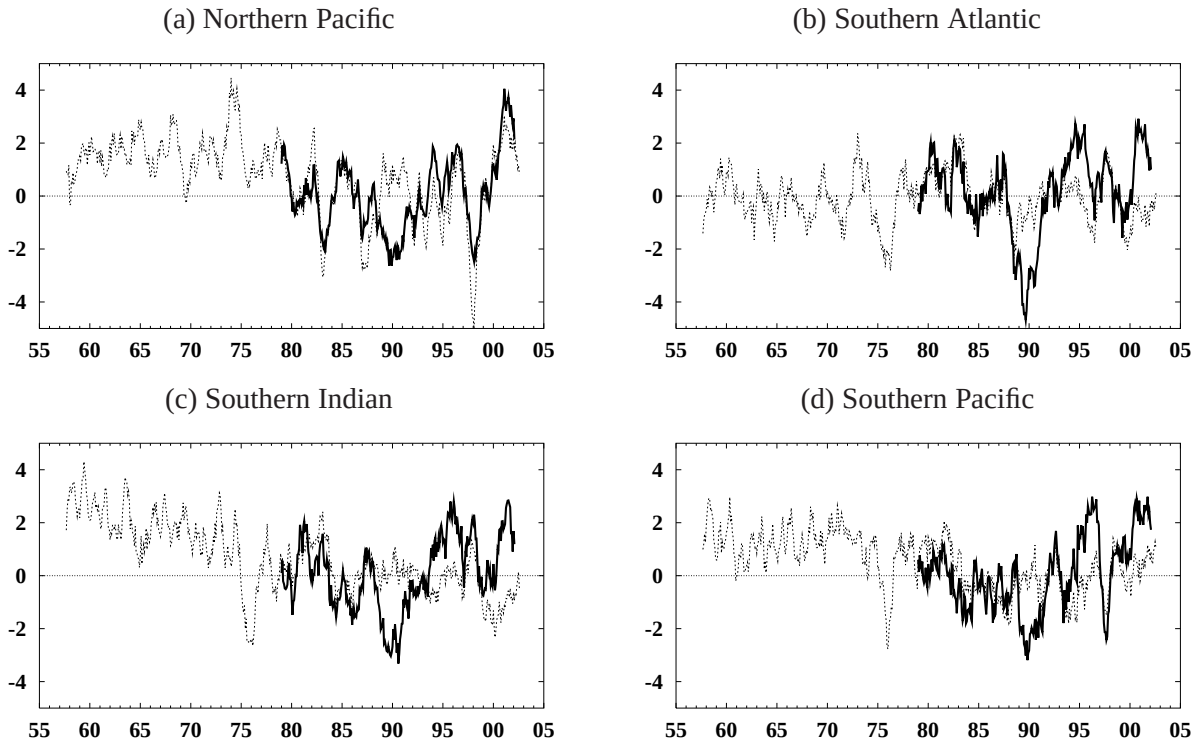

Figure 12: Same as Fig. 11 for the last four maritime regions of Table 1.

(a) January

(b) July

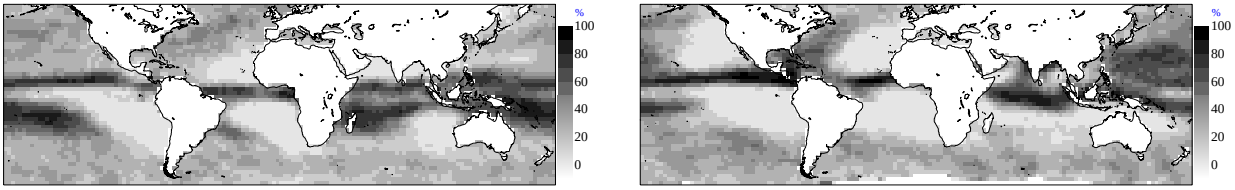

Figure 13: Mean frequency of high clouds from the climate run for January and July between July 1983 and September 2001. High clouds are detected from the cloud ice profiles.

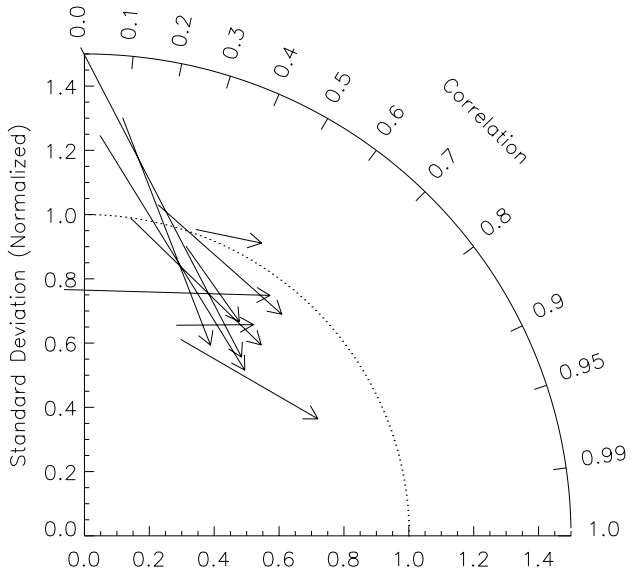

Figure 14: Polar representation of normalised standard deviations (radius) vs. correlations (angle) between the high cloud frequency anomalies from HIRS and the climate run (tail of the arrows) or ERA-40 12-hour forecasts (head of the arrows). For the climate run as for ERA-40, high clouds are detected from the cloud ice profiles. Monthly anomalies are defined for each dataset with respect to its July 1983 - September 2001 climatology. Statistics are computed for the ten maritime regions of Table 1, but for clarity the arrows are not labelled.

(a) January

(b) July

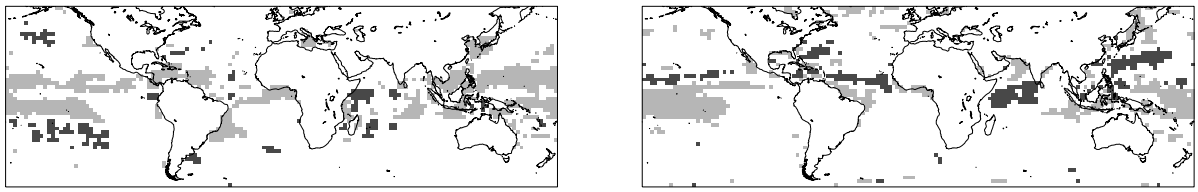

Figure 15: Difference in high cloud occurrence between ERA-40 36-hour forecast started at 00 and 12 UTC and the corresponding 00 and 12 UTC analysis for January and July between July 1983 and September 2001. Values larger (respectively smaller) than 3% (respectively -3%) are dark (respectively light) shaded. High clouds are detected from the cloud ice profiles.